
Differentially Private Mean Embeddings with Random Features for Synthetic Data Generation

Frederik Harder^{*,1,2}, Kamil Adamczewski^{*,1,3}, Mijung Park^{1,2}

^{*}Equal Contribution

¹Max Planck Institute for Intelligent Systems

²University of Tübingen

³ETH Zürich

{fharder|kadamczewski|mpark}@tue.mpg.de

Abstract

We present a differentially private data generation paradigm using random feature representations of kernel mean embeddings when comparing the distribution of true data with that of synthetic data. We exploit the random feature representations for two important benefits. First, we require a very low privacy cost for training deep generative models. This is because unlike kernel-based distance metrics that require computing the kernel matrix on all pairs of true and synthetic data points, we can detach the data-dependent term from the term solely dependent on synthetic data. Hence, we need to perturb the data-dependent term once-for-all and then use it until the end of the generator training. Second, we can obtain an *analytic* sensitivity of the kernel mean embedding as the random features are norm bounded by construction. This removes the necessity of hyper-parameter search for a clipping norm to handle the unknown sensitivity of a generator network. We provide several variants of our algorithm, *differentially-private mean embeddings with random features* (DP-MERF) to jointly generate labels and input features for datasets such as heterogeneous tabular data and image data. Our algorithm achieves better privacy-utility trade-offs than existing methods when tested on several datasets.

1 Introduction

Differential privacy (DP) is a gold standard privacy notion that is widely used in many applications in machine learning. However, due to its composability, every access to data reduces the privacy guarantee, which limits the number of times to query sensitive data until a desired privacy level is met. Differentially private data generation solves this problem of limited access by creating a synthetic dataset that is *similar* to the true dataset using DP mechanisms. This process also comes at a privacy cost, but afterwards, the synthetic dataset can be used in place of the true one for unlimited time without further loss of privacy.

Classical approaches to differentially private data generation typically assume a certain class of pre-specified queries. These DP algorithms produce a privacy-preserving synthetic database that is similar to the privacy-sensitive original data for that *fixed query class* [10, 13, 26, 30]. However, specifying a query class upfront significantly limits the flexibility of the synthetic data, if data analysts hope to perform other machine learning tasks.

To overcome this inflexibility, many papers on DP data generation have utilized the recent advances in deep generative modeling. The majority of these approaches is based on the generative adversarial networks (GAN) [8] framework, where a discriminator and a generator play a min-max form of game to optimize a given distance metric between the true and synthetic data distributions. Most

approaches have used either the *Jensen-Shannon divergence* [16, 23, 28], or the Wasserstein distance [6, 27]. For more details on different divergence metrics, see Appendix A.

Another popular choice of distance metric for generative modelling is Maximum Mean Discrepancy (MMD). MMD compares two probability measures in terms of all possible moments, resulting in no information loss due to a selection of a certain set of moments. The MMD estimator is in closed form (eq. 1) and easy to compute by the pair-wise evaluations of a kernel function using the points drawn from the true and the generated data distributions.

In this work, we propose to use a particular form of MMD via *random Fourier feature* representations [17] of kernel mean embeddings for DP data generation. While MMD can be used within a GAN framework as well (see e.g. [11, 12]) we choose a much simpler method, which is particularly suited for training with DP constraints. The random feature representations of mean embeddings (eq. 2) we use as an objective separate the mean embedding of the true data distribution (data-dependent) from that of the synthetic data distribution (data-independent). Hence, only the data-dependent term requires privatization. Random features provide an analytic sensitivity of the mean embedding, which allows us to release a DP version of this embedding through a DP mechanism as we explain below. With the privatized data embedding and the synthetic data embedding, our objective no longer directly accesses the data and can be optimized freely to train a data generator. Our contributions are summarized below.

(1) We provide a simple algorithm for DP data generation, which improves on existing methods both in privacy and utility.

- *Simple to optimize*: Our method avoids the cumbersome min-max optimization, which often results in high cost computations to find the right setup. This exacerbates with more hyperparameters such as empirical sensitivities present in GAN based approaches. Our method requires only minimization with a minimal number of hyperparameters¹.
- *Strong privacy*: By requiring only a single DP-release which has an analytic sensitivity, our method can provide strong DP guarantee more easily than methods which access the data on each training iteration.
- *High utility*: Since the objective is already made private, the optimization is not constrained in any way, which leads to better results. This contrast is particularly stark on MNIST, where our model at a strong privacy guarantee of $(0.2, 10^{-5})$ -DP outperforms DP-CGAN with a weak privacy of $(9.6, 10^{-5})$ -DP by over 10%.

(2) Our algorithm accommodates several needs in privacy-preserving data generation.

- *Generating input and output pairs jointly*: We treat both input and output to be privacy-sensitive. This is different from the conditional-GAN type of methods, where the class distribution is treated as non-sensitive, which increases the risk of identification, particularly in imbalanced datasets where some classes contain only a small number of samples.
- *Generating imbalanced and heterogeneous tabular data*: This is an important condition for a DP method to be useful, as real world datasets frequently exhibit class-imbalance and heterogeneity.

We start by describing necessary background information in Sec. 2 before introducing our method in Sec. 3, followed by an overview of related work in Sec. 4 and experiments in Sec. 5.

2 Background

In the following, we describe the kernel mean embeddings with random features, and introduce differential privacy, which our model will use in Sec. 3.

¹Hyperparameters in our method are the number of random features, a kernel parameter, and the learning rate.

2.1 Random feature mean embeddings

Given the samples drawn from two probability distributions: $X_m = \{x_i\}_{i=1}^m \sim P$ and $X'_n = \{x'_i\}_{i=1}^n \sim Q$, the MMD biased estimator is defined as [9]:

$$\widehat{\text{MMD}}^2(X_m, X'_n) = \frac{1}{m^2} \sum_{i,j=1}^m k(x_i, x_j) + \frac{1}{n^2} \sum_{i,j=1}^n k(x'_i, x'_j) - \frac{2}{mn} \sum_{i=1}^m \sum_{j=1}^n k(x_i, x'_j). \quad (1)$$

The total computational cost of $\widehat{\text{MMD}}(X_m, X'_n)$ is $O(mn)$, which is prohibitive for large-scale datasets. A fast linear-time MMD estimator can be achieved by considering an approximation to the kernel function $k(x, x')$ with an inner product of finite dimensional feature vectors, i.e., $k(x, x') \approx \hat{\phi}(x)^\top \hat{\phi}(x')$ where $\hat{\phi}(x) \in \mathbb{R}^D$ and D is the number of features. The resulting approximation of the MMD estimator given in eq. 1 is

$$\widehat{\text{MMD}}_{rf}^2(P, Q) = \left\| \frac{1}{m} \sum_{i=1}^m \hat{\phi}(x_i) - \frac{1}{n} \sum_{i=1}^n \hat{\phi}(x'_i) \right\|_2^2, \quad (2)$$

which can be computed in $O(m + n)$, i.e., linear in the sample size. One popular approach to obtaining such $\hat{\phi}(\cdot)$ is based on random Fourier features [17] which can be applied to any translation invariant kernel, i.e., $k(x, x') = \tilde{k}(x - x')$ for some function \tilde{k} . According to Bochner's theorem [18], \tilde{k} can be written as $\tilde{k}(x - x') = \int e^{i\omega^\top(x-x')} d\Lambda(\omega) = \mathbb{E}_{\omega \sim \Lambda} \cos(\omega^\top(x - x'))$, where $i = \sqrt{-1}$ and due to positive-definiteness of \tilde{k} , its Fourier transform Λ is nonnegative and can be treated as a probability measure. By drawing random frequencies $\{\omega_i\}_{i=1}^D \sim \Lambda$, where Λ depends on the kernel, (e.g., a Gaussian kernel k corresponds to normal distribution Λ), $\tilde{k}(x - x')$ can be approximated with a Monte Carlo average. The vector of random Fourier features is given by

$$\hat{\phi}(x) = (\hat{\phi}_1(x), \dots, \hat{\phi}_D(x))^\top \quad (3)$$

where each coordinate is defined by

$$\begin{aligned} \hat{\phi}_j(x) &= \sqrt{2/D} \cos(\omega_j^\top x), \\ \hat{\phi}_{j+D/2}(x) &= \sqrt{2/D} \sin(\omega_j^\top x), \end{aligned}$$

for $j = 1, \dots, D/2$. The approximation error of these random features is studied in [20].

2.2 Differential privacy

Given privacy parameters $\epsilon \geq 0$ and $\delta \geq 0$, a mechanism \mathcal{M} is (ϵ, δ) -DP if and only if for all possible sets of mechanism outputs S and all neighbouring datasets $\mathcal{D}, \mathcal{D}'$ differing by a single entry, the following equation holds:

$$\Pr[\mathcal{M}(\mathcal{D}) \in S] \leq e^\epsilon \cdot \Pr[\mathcal{M}(\mathcal{D}') \in S] + \delta \quad (4)$$

A DP mechanism guarantees a limit on the amount of information revealed about any one individual in the dataset. Typically this guarantee is achieved by adding randomness to the algorithms' output. Let a function $h : \mathcal{D} \mapsto \mathbb{R}^p$ computed on sensitive data \mathcal{D} output a p -dimensional vector. We can add noise to h for privacy, where the level of noise is calibrated to the *global sensitivity* [5], Δ_h , defined by the maximum difference in terms of L_2 -norm $\|h(\mathcal{D}) - h(\mathcal{D}')\|_2$, for neighboring \mathcal{D} and \mathcal{D}' (i.e. differ by one data sample). The *Gaussian mechanism* that we will use in this paper outputs $\tilde{h}(\mathcal{D}) = h(\mathcal{D}) + \mathcal{N}(0, \sigma^2 \Delta_h^2 \mathbf{I}_p)$. The perturbed function $\tilde{h}(\mathcal{D})$ is (ϵ, δ) -DP, where σ is a function of ϵ and δ .

There are two important properties of DP. The *composability* theorem [5] states that the strength of privacy guarantee degrades in a measurable way with repeated use of DP-algorithms. This allows us to combine the results of different private mechanisms in Sec. 3.1. Furthermore, the *post-processing invariance* property [5] tells us that the composition of any arbitrary data-independent mapping with an (ϵ, δ) -DP algorithm is also (ϵ, δ) -DP. This ensures that no analysis of the released synthetic data can yield more information about the real data than our choice of ϵ and δ allow.

3 Differentially private mean embeddings with random features

We first introduce the DP-MERF algorithm to learn the joint² distribution over the input features \mathbf{x} and output labels \mathbf{y} (either categorical variables in classification, or numerical variables in regression). The benefit of learning the joint distribution is that we do not need to assume the information on the output labels to be public. By learning the joint distribution, we keep the ratio of the datapoints across different classes the same in the generated dataset as in the real dataset. This way our generated dataset is truthful to the privacy-sensitive original dataset in terms of the distribution over both input features and output labels.

3.1 DP-MERF for input/output pairs

Suppose a generator G_θ (parameterized by θ) takes a pair of inputs $\mathbf{z}_x, \mathbf{z}_y$ drawn from a known distribution and outputs a pair of samples denoted by $\tilde{\mathbf{x}}_\theta, \tilde{\mathbf{y}}_\theta : G_\theta(\mathbf{z}_x, \mathbf{z}_y) \mapsto (\tilde{\mathbf{x}}_\theta, \tilde{\mathbf{y}}_\theta)$. We consider the following objective function,

$$\widehat{\text{MMD}}_{rf}^2(P_{\mathbf{x}, \mathbf{y}}, Q_{\tilde{\mathbf{x}}_\theta, \tilde{\mathbf{y}}_\theta}) = \left\| \widehat{\boldsymbol{\mu}}_{P_{\mathbf{x}, \mathbf{y}}} - \widehat{\boldsymbol{\mu}}_{Q_{\mathbf{x}, \mathbf{y}}} \right\|_F^2, \quad (5)$$

where F denotes the Frobenius norm. This type of joint maximum mean discrepancy was used in other papers [7, 29].

We compose $P_{\mathbf{x}, \mathbf{y}} = P_{\mathbf{x}|\mathbf{y}} P_{\mathbf{y}}$, and the generator accordingly: $G = G_1 \circ G_2$, where $G_2(\mathbf{z}_y) \mapsto \tilde{\mathbf{y}}$ and $G_1(\mathbf{z}_x|\tilde{\mathbf{y}}) \mapsto \tilde{\mathbf{x}}$. Here we consider a kernel from a product of two existing kernels, $k((\mathbf{x}, \mathbf{y}), (\mathbf{x}', \mathbf{y}')) = k_x(\mathbf{x}, \mathbf{x}') k_y(\mathbf{y}, \mathbf{y}')$, where k_x is a kernel for input features and k_y is a kernel for output labels. For regression, we could use the Gaussian kernel for both k_x and k_y . For classification, we could use the Gaussian kernel for k_x and the polynomial kernel with order-1, $k_y(\mathbf{y}, \mathbf{y}') = \mathbf{y}^\top \mathbf{y}' + c$ for one-hot-encoded labels \mathbf{y} and some constant c , for instance.³ In this case, the resulting kernel is also characteristic, forming the corresponding MMD as a metric, as explained in [21]. We represent the mean embeddings using random features

$$\begin{aligned} \widehat{\boldsymbol{\mu}}_{P_{\mathbf{x}, \mathbf{y}}} &= \frac{1}{m} \sum_{i=1}^m \widehat{\mathbf{f}}(\mathbf{x}_i, \mathbf{y}_i), \text{ for true data} \\ \widehat{\boldsymbol{\mu}}_{Q_{\mathbf{x}, \mathbf{y}}} &= \frac{1}{n} \sum_{i=1}^n \widehat{\mathbf{f}}(G_\theta(\mathbf{z}_{\mathbf{x}_i}, \mathbf{z}_{\mathbf{y}_i})), \text{ for synthetic data} \end{aligned} \quad (6)$$

where we define $\widehat{\mathbf{f}}(\mathbf{x}_i, \mathbf{y}_i) := \text{vec}(\widehat{\phi}(\mathbf{x}_i) \mathbf{f}(\mathbf{y}_i)^\top)$, where $\mathbf{f}(\mathbf{y}_i) = \mathbf{y}_i$ for the order-1 polynomial kernel and \mathbf{y}_i is one-hot-encoded. See Appendix B for derivation. As a matrix notation, the random feature mean embedding in eq. 6 can be also written as $\widehat{\boldsymbol{\mu}}_{P_{\mathbf{x}, \mathbf{y}}} = [\mathbf{m}_1, \dots, \mathbf{m}_C] \in \mathbb{R}^{D \times C}$ where the c 'th column is defined by

$$\mathbf{m}_c = \frac{1}{m} \sum_{i \in c}^{m_c} \widehat{\phi}(\mathbf{x}_i) \quad (7)$$

where c is the set of the datapoints that belong to the class c , and m_c is the number of those datapoints. Recall that D is the number of random features. C is the number of classes in the dataset. Notice that the sum in each column is over the number of instances that belong to the particular class c , while the divisor is the number of samples in the entire dataset, m . This brings difficulties in learning with this loss function when classes are highly imbalanced, as for rare classes m can be significantly larger than the sum of the corresponding column. Hence, for class-imbalanced datasets, we modify the mean embedding by appropriately weighting it⁴: $\tilde{\boldsymbol{\mu}}_{P_{\mathbf{x}, \mathbf{y}}} = [\frac{1}{\omega_1} \mathbf{m}_1, \dots, \frac{1}{\omega_C} \mathbf{m}_C]$ where the

²Using DP-MERF to learn the distribution over the input features only for unsupervised learning is trivial: it is sufficient to replace the mean embeddings of the joint distribution with those of the marginal distribution over the input features.

³The optimal choice of Kernel requires knowledge on the characteristics of the data (see guidelines in Ch. 4 in [25]). At small data sample sizes, a bad kernel choice will affect the efficiency of the algorithm and can underestimate MMD if the chosen kernel assigns small weights to the “correct” frequencies at which the distributions differ. However, with a large enough sample, any characteristic kernel is able to capture such differences.

⁴We arrive at this expression if we modify the kernel on the labels by a weighted one, i.e., $k_y(\mathbf{y}, \mathbf{y}') = \sum_{c=1}^C \frac{1}{\omega_c} \mathbf{y}_c^\top \mathbf{y}'_c$.

Algorithm 1 DP-MERF for generating input/output pairs

Require: Dataset \mathcal{D} , and a privacy level (ϵ, δ)

Ensure: (ϵ, δ) -DP input output samples for all classes

Step 1. Given (ϵ, δ) , compute the privacy parameter σ by the RDP composition in [24] for the $(C + 1)$ repeated use of the Gaussian mechanism.

Step 2. Privatize the random feature mean embeddings via $\mathcal{M}_{weights}$ and $\mathcal{M}_{\mathbf{m}_c}$.

Step 3. Train the generator by minimizing eq. 11

vector of weights is defined by

$$\boldsymbol{\omega} = [\omega_1, \dots, \omega_C], \quad (8)$$

and $\omega_c = \frac{m_c}{m}$. By dividing by the weights, now each column has a similar order of strength regardless of the number of datapoints belonging to the specific class. Here we privatize the weights $\boldsymbol{\omega}$ and each column \mathbf{m}_c separately, using the two mechanisms defined below.

Definition 3.1 ($\mathcal{M}_{weights}$) *The mechanism takes a dataset \mathcal{D} and computes eq. 8. It outputs the privatized weights given a privacy parameter σ , the number of classes C and the sensitivity $\Delta_{\boldsymbol{\omega}}$.*

$$\tilde{\boldsymbol{\omega}} = \boldsymbol{\omega} + \mathcal{N}(0, \sigma^2(\Delta_{\boldsymbol{\omega}})^2 \mathbf{I}_C), \quad (9)$$

Note that privatizing weight vector is analogous to privatizing the mixing coefficients in [15]. If there is one datapoint's difference in the neighbouring two datasets, only two elements can differ in the weight vector, resulting in the sensitivity of $\Delta_{\boldsymbol{\omega}} = \frac{\sqrt{2}}{m}$. These DP weights become the inputs \mathbf{z}_y to the generator for label generation: $G_2(\tilde{\boldsymbol{\omega}}) \mapsto \tilde{\mathbf{y}}$ to sample the output labels according to the real dataset.

Definition 3.2 ($\mathcal{M}_{\mathbf{m}_c}$) *The mechanism takes a dataset \mathcal{D} and computes eq. 7. It outputs the privatized quantity given a privacy parameter σ , the number of random features D and the sensitivity $\Delta_{\mathbf{m}_c}$,*

$$\tilde{\mathbf{m}}_c = \mathbf{m}_c + \mathcal{N}(0, \sigma^2(\Delta_{\mathbf{m}_c})^2 \mathbf{I}_D) \quad (10)$$

As the norm of $\hat{\phi}$ is bounded by 1, the sensitivity of \mathbf{m}_c (eq. 7) is $\Delta_{\mathbf{m}_c} = \frac{2}{m}$. During the training, we will need to perform $\mathcal{M}_{weights}$ once, and $\mathcal{M}_{\mathbf{m}_c}$ as many times as the number of classes. Hence, we divide our privacy budget into $C + 1$ compositions of the Gaussian mechanisms. Now the objective function to minimize is modified to

$$\widehat{\text{MMD}}_{rf}^2(P_{\mathbf{x}, \mathbf{y}}^{DP}, Q_{\tilde{\mathbf{x}}_{\theta}, \tilde{\mathbf{y}}_{\theta}}) = \left\| \tilde{\boldsymbol{\mu}}_{P_{\mathbf{x}, \mathbf{y}}}^{DP} - \hat{\boldsymbol{\mu}}_{Q_{\mathbf{x}, \mathbf{y}}} \right\|_2^2, \quad (11)$$

where $\tilde{\boldsymbol{\mu}}_{P_{\mathbf{x}, \mathbf{y}}}^{DP} = \left[\frac{1}{\omega_1} \tilde{\mathbf{m}}_1, \dots, \frac{1}{\omega_C} \tilde{\mathbf{m}}_C \right]$. Our algorithm is summarized in Algorithm 1.

Note that by privatizing the weights and each column \mathbf{m}_c separately, we can get the benefit of sensitivity being on the order of $1/m$, rather than on the order of $1/m_c$ where the latter could hamper the training performance as in highly imbalanced datasets m_c can be very small resulting in a high additive noise variance.

3.2 DP-MERF for heterogeneous data

To handle heterogeneous data consisting of continuous variables denoted by \mathbf{x}_{con} and discrete variables denoted by \mathbf{x}_{dis} , we consider the sum of two existing kernels, $k((\mathbf{x}_{con}, \mathbf{x}_{dis}), (\mathbf{x}'_{con}, \mathbf{x}'_{dis})) = k_{con}(\mathbf{x}_{con}, \mathbf{x}'_{con}) + k_{dis}(\mathbf{x}_{dis}, \mathbf{x}'_{dis})$, where k_{con} is a kernel for continuous variables and k_{dis} is a kernel for discrete variables. Note that this does not mean that we assume independence of the two types of variables explicitly, for details see Appendix H.

As before, we could use the Gaussian kernel for $k_{con}(\mathbf{x}_{con}, \mathbf{x}'_{con}) = \hat{\phi}(\mathbf{x}_{con})^{\top} \hat{\phi}(\mathbf{x}'_{con})$ and a normalized polynomial kernel with order-1, $k_{dis}(\mathbf{x}_{dis}, \mathbf{x}'_{dis}) = \frac{1}{d_{dis}} \mathbf{x}_{dis}^{\top} \mathbf{x}'_{dis}$ for one-hot-encoded

values \mathbf{x}_{dis} and the length of \mathbf{x}_{dis} being d_{dis} . This normalization is to match the importance of the two kernels in the resulting mean embeddings. Under these kernels, we can approximate the mean embeddings using random features

$$\hat{\boldsymbol{\mu}}_{P_{\mathbf{x}}} = \frac{1}{m} \sum_{i=1}^m \hat{\mathbf{h}}(\mathbf{x}_{con}^{(i)}, \mathbf{x}_{dis}^{(i)}), \quad (12)$$

where we define $\hat{\mathbf{h}}(\mathbf{x}_{con}^{(i)}, \mathbf{x}_{dis}^{(i)}) := \begin{bmatrix} \hat{\phi}(\mathbf{x}_{con}^{(i)}) \\ \frac{1}{\sqrt{d_{dis}}} \mathbf{x}_{dis}^{(i)} \end{bmatrix}$ from the definition of kernel (See Appendix C for derivation). In summary, for generating input and output pairs jointly when the input features are heterogeneous, we run Algorithm 1 with three changes: (a) redefine $\hat{\mathbf{f}}(\mathbf{x}, \mathbf{y})$ in eq. 6 as $\text{vec}(\hat{\mathbf{h}}(\mathbf{x}_{con}, \mathbf{x}_{dis}) \mathbf{f}(\mathbf{y})^\top)$; (b) redefine \mathbf{m}_c in eq. 10 as $\frac{1}{m} \sum_{i \in c}^m \hat{\mathbf{h}}(\mathbf{x}_i)$; and (c) change the sensitivity of \mathbf{m}_c to $\Delta_{\mathbf{m}_c} = \frac{2\sqrt{2}}{m}$ (see Appendix F for proof).

4 Related work

There are two categories of prior work that are relevant to ours. The first category is the differentially private GAN framework and its variants [6, 23, 27, 28]. The core technique of most of these algorithms is based on DP-SGD, with an exception that [28] is based on the Private Aggregation of Teacher Ensembles (PATE). Unlike these methods, our method does not involve the difficult task of finding the equilibrium between the generator and the discriminator. Our method is not limited to the binary classification problems as in PATE-GAN [28]; nor requires a complicated sensitivity computation as in DP-GAN [27]. Furthermore, our method can produce input and output pairs jointly for supervised learning problems. DP-CGAN [23] generates the input features conditioning on the labels, while it does not learn the distribution over the labels. The only method we are aware of aiming at generating data for multi-class supervised learning is DP-CGAN, against which we will compare our method in Sec. 5.

The second category is the framework of kernel methods with differential privacy. [3] proposed to use the reduced set method in conjunction with random features for sharing DP mean embeddings, but generative models are not part of their algorithms. [19] also used the random feature representations of the mean embeddings for the DP distributed data summarization to take into account covariate shifts.

Table 1: Performance comparison on Tabular datasets. The average over five runs.

	Real		DP-CGAN (1, 10 ⁻⁵)-DP		DP-GAN (1, 10 ⁻⁵)-DP		DP-MERF (1, 10 ⁻⁵)-DP		DP-MERF (non-priv)	
adult	ROC	PRC	ROC	PRC	ROC	PRC	ROC	PRC	ROC	PRC
census	0.730	0.639	0.509	0.444	0.511	0.445	0.650	0.564	0.653	0.570
cervical	0.747	0.415	0.655	0.216	0.529	0.166	0.686	0.358	0.692	0.369
credit	0.786	0.493	0.519	0.200	0.485	0.183	0.545	0.184	0.896	0.737
epileptic	0.923	0.874	0.664	0.356	0.435	0.150	0.772	0.637	0.898	0.774
isolet	0.797	0.617	0.578	0.241	0.505	0.196	0.611	0.340	0.616	0.335
	0.893	0.728	0.511	0.198	0.540	0.205	0.547	0.404	0.733	0.424
	F1		F1		F1		F1		F1	
covtype	0.643		0.285		0.492		0.467		0.513	
intrusion	0.959		0.302		0.251		0.85		0.856	

5 Experiments

The experiments present robustness of the method in producing a diverse range of data both in private and non-private settings. We first train a generator using either DP-MERF or a comparison method, and obtain *synthetic* data samples, which we use to train 12 predictive models (see Table 5 in the Appendix for the models). We then evaluate these trained models using the synthetic data to predict

the labels of *real* test data. This evaluation follows [28], but note that hyper-parameters of the 12 models differ because the exact settings used in [28] were not available to us, which means that their scores are not directly comparable to ours. For comparison, we test DP-CGAN [23], as well as our own implementation of an ensemble of 10 DP-GANs, where each model generates data for one class. Our version of DP-GAN differs from [27] in that it uses standard DP-SGD [1] with gradient clipping rather than weight clipping. The results in [27, 28] could not be reproduced as the released code was incomplete.

As comparison metrics, we use ROC (area under the receiver operating characteristics curve) and PRC (area under the precision recall curve) for binary-labeled data. We use F1 score and prediction accuracy for multiclass-labeled data. As a baseline, we also show the performance of the models trained with the real training data. All the numbers shown in the tables are the average over 5 independent runs. Due to the space limit, we describe all our experimental details (e.g., architecture choices for generators, chosen number of random features, etc.) in the Appendix.

Heterogeneous tabular data We begin the experiments with a set of tabular data which contain real-world information. The datasets we consider contain either only numerical data (homogenous) or both numerical and categorical data (including ordinal data such as education), which we call heterogenous datasets. The numerical features which are both discrete and continuous values. The categorical features can have two classes (e.g. whether a person smokes or not) or several classes (e.g. country of origin). The output labels are also categorical; we include datasets with both binary and multiclass labels. Table 2 summarizes the datasets. Table 1 shows the average across the 12 predictive models trained by the generated samples from DP-CGAN, DP-GAN and DP-MERF. Results for the individual models can be found in Appendix K. DP-MERF produces high-quality samples which are only a few percentage points short of the real-world data. The method works well both with numerical and categorical data. In the private setting, we perturb the mean embedding of the true data once using Algorithm 1, resulting in a relatively small drop in evaluation metrics.

Image data For image datasets, MNIST and FashionMNIST, two changes are made to the training procedure of DP-MERF generators. Firstly, as the datasets in question are almost perfectly balanced, we assume that the label distribution is uniform instead of learning it. Secondly, the generator architecture is changed to include convolutional layers, alternating with bilinear upsampling, to take advantage of the inherent structure of image data.

Table 3: Test accuracy on image data. In all cases $\delta = 10^{-5}$.

	Real	DP-CGAN $\epsilon = 9.6$	DP-GAN $\epsilon = 9.6$	DP-MERF $\epsilon = \infty$	DP-MERF $\epsilon = 1$	DP-MERF $\epsilon = 0.2$
MNIST	0.87	0.50	0.48	0.65	0.65	0.61
FashionMNIST	0.78	0.39	0.46	0.61	0.62	0.53

Table 3 compares the real data prediction performance based generated training sets using all three models. Results are averaged over 12 classifiers. It shows that DP-MERF outperforms the GAN based methods by a wide margin and maintains good performance under more meaningful privacy constraints of $(1, 10^{-5})$ -DP and $(0.2, 10^{-5})$ -DP. Looking at the generated samples of the three tested methods in Fig. 1, we see that the samples from DP-MERF at $\epsilon = 0.2$ are noisier than those of DP-CGAN, while still achieving higher downstream accuracy. This indicates that the distinctive features of the data are preserved despite the noisy appearance of the DP-MERF samples. In addition, a difference in sample diversity may be responsible.

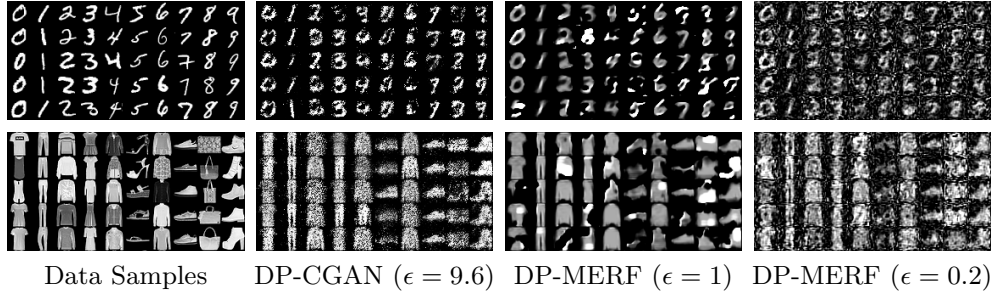


Figure 1: Generated samples with different levels of privacy

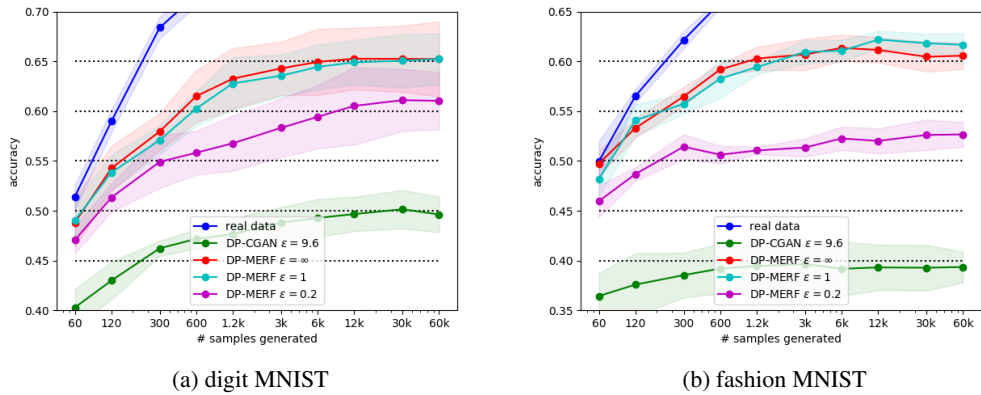


Figure 2: Test accuracy of classifiers trained on synthetic datasets of varying size. Scores are averaged over 12 models and 5 random seeds. Confidence intervals denote ± 1 standard deviation.

Sample diversity We investigate how diverse the generated data samples are in DP-MERF and DP-CGAN. For quantifying the diversity, we trained models using generated datasets of varying size from 60 to 60,000 samples and comparing the accuracy classifiers trained on these datasets. In Fig. 2 (Left for MNIST digits), we see that all models show the increase in accuracy as we increase the number of sample size from 60 to 12K. However, more than 12K samples, we do not see any increase in the classification accuracy, indicating the lack of diversity from this size on. On the other hand, in Fig. 2 (Right for Fashion-MNIST), this exacerbates as the complexity of data increases. The take-away message from this evaluation is that the models we tested including ours need to improve to be able to faithfully express the inherent complexity and the diversity of the data.

6 Summary and Discussion

We proposed a simple and practical algorithm using the random feature representation of kernel mean embeddings for DP data generation. Our method requires a significantly lower privacy budget to produce quality data samples compared to GAN based approaches, tested on 8 tabular datasets and 2 image datasets. The metrics we used were targeting at supervised learning tasks, but the method is not limited to this application. In future work, we plan to evaluate our method on a more diverse set of tasks and expand it, to scale to more complex data.

References

[1] M. Abadi, A. Chu, I. Goodfellow, H. B. McMahan, I. Mironov, K. Talwar, and L. Zhang. “Deep Learning with Differential Privacy”. In: *Proceedings of the 2016 ACM SIGSAC Conference on Computer and Communications Security*. CCS ’16. New York, NY, USA: Association for Computing Machinery, 2016, pp. 308–318.

[2] M. Arjovsky, S. Chintala, and L. Bottou. “Wasserstein GAN”. In: *ArXiv* abs/1701.07875 (2017).

[3] M. Balog, I. Tolstikhin, and B. Schölkopf. “Differentially Private Database Release via Kernel Mean Embeddings”. In: *Proceedings of the 35th International Conference on Machine Learning (ICML)*. Vol. 80. Proceedings of Machine Learning Research. PMLR, July 2018, pp. 423–431.

[4] I. Csiszár and P. Shields. “Information Theory and Statistics: A Tutorial”. In: *Foundations and Trends® in Communications and Information Theory* 1.4 (2004), pp. 417–528.

[5] C. Dwork, K. Kenthapadi, F. McSherry, I. Mironov, and M. Naor. “Our Data, Ourselves: Privacy Via Distributed Noise Generation.” In: *Eurocrypt*. Vol. 4004. Springer. 2006, pp. 486–503.

[6] L. Frigerio, A. S. de Oliveira, L. Gomez, and P. Duverger. “Differentially Private Generative Adversarial Networks for Time Series, Continuous, and Discrete Open Data”. In: *ICT Systems Security and Privacy Protection - 34th IFIP TC 11 International Conference, SEC 2019, Lisbon, Portugal, June 25-27, 2019, Proceedings*. 2019, pp. 151–164.

[7] H. Gao and H. Huang. “Joint Generative Moment-Matching Network for Learning Structural Latent Code”. In: *Proceedings of the Twenty-Seventh International Joint Conference on Artificial Intelligence, IJCAI-18*. International Joint Conferences on Artificial Intelligence Organization, July 2018, pp. 2121–2127.

[8] I. Goodfellow, J. Pouget-Abadie, M. Mirza, B. Xu, D. Warde-Farley, S. Ozair, A. Courville, and Y. Bengio. “Generative Adversarial Nets”. In: *Advances in Neural Information Processing Systems 27*. Ed. by Z. Ghahramani, M. Welling, C. Cortes, N. D. Lawrence, and K. Q. Weinberger. Curran Associates, Inc., 2014, pp. 2672–2680.

[9] A. Gretton, K. M. Borgwardt, M. J. Rasch, B. Schölkopf, and A. Smola. “A kernel two-sample test”. In: *Journal of Machine Learning Research* 13.Mar (2012), pp. 723–773.

[10] M. Hardt, K. Ligett, and F. Mcsherry. “A Simple and Practical Algorithm for Differentially Private Data Release”. In: *Advances in Neural Information Processing Systems 25*. Ed. by F. Pereira, C. J. C. Burges, L. Bottou, and K. Q. Weinberger. Curran Associates, Inc., 2012, pp. 2339–2347.

[11] C.-L. Li, W.-C. Chang, Y. Cheng, Y. Yang, and B. Poczos. “MMD GAN: Towards Deeper Understanding of Moment Matching Network”. In: *Advances in Neural Information Processing Systems 30*. Ed. by I. Guyon, U. V. Luxburg, S. Bengio, H. Wallach, R. Fergus, S. Vishwanathan, and R. Garnett. Curran Associates, Inc., 2017, pp. 2203–2213.

[12] C.-L. Li, W.-C. Chang, Y. Cheng, Y. Yang, and B. Póczos. “MMD GAN: Towards Deeper Understanding of Moment Matching Network”. In: *Proceedings of the 31st International Conference on Neural Information Processing Systems*. NIPS’17. Red Hook, NY, USA: Curran Associates Inc., 2017, pp. 2200–2210.

[13] N. Mohammed, R. Chen, B. C. Fung, and P. S. Yu. “Differentially Private Data Release for Data Mining”. In: *Proceedings of the 17th ACM SIGKDD International Conference on Knowledge Discovery and Data Mining*. KDD ’11. New York, NY, USA: ACM, 2011, pp. 493–501.

[14] S. Nowozin, B. Cseke, and R. Tomioka. “f-GAN: Training Generative Neural Samplers Using Variational Divergence Minimization”. In: *Proceedings of the 30th International Conference on Neural Information Processing Systems*. NIPS’16. USA: Curran Associates Inc., 2016, pp. 271–279.

[15] M. Park, J. Foulds, K. Choudhary, and M. Welling. “DP-EM: Differentially Private Expectation Maximization”. In: *Proceedings of the 20th International Conference on Artificial Intelligence and Statistics*. Ed. by A. Singh and J. Zhu. Vol. 54. Proceedings of Machine Learning Research. Fort Lauderdale, FL, USA: PMLR, Apr. 2017, pp. 896–904.

[16] N. Park, M. Mohammadi, K. Gorde, S. Jajodia, H. Park, and Y. Kim. “Data Synthesis Based on Generative Adversarial Networks”. In: *Proc. VLDB Endow.* 11.10 (June 2018), pp. 1071–1083.

[17] A. Rahimi and B. Recht. “Random features for large-scale kernel machines”. In: *Advances in neural information processing systems*. 2008, pp. 1177–1184.

[18] W. Rudin. *Fourier Analysis on Groups: Interscience Tracts in Pure and Applied Mathematics*, No. 12. English. Literary Licensing, LLC, 2013.

- [19] K. Sarpatwar, K. Shanmugam, V. S. Ganapavarapu, A. Jagmohan, and R. Vaculin. “Differentially Private Distributed Data Summarization under Covariate Shift”. In: *Advances in Neural Information Processing Systems*. 2019, pp. 14432–14442.
- [20] D. J. Sutherland and J. Schneider. “On the Error of Random Fourier Features”. In: *Proceedings of the Thirty-First Conference on Uncertainty in Artificial Intelligence*. UAI’15. Arlington, Virginia, USA: AUAI Press, 2015, pp. 862–871.
- [21] Z. Szabó and B. K. Sriperumbudur. “Characteristic and Universal Tensor Product Kernels”. In: *Journal of Machine Learning Research* 18.233 (2018), pp. 1–29.
- [22] I. Tolstikhin, O. Bousquet, S. Gelly, and B. Schoelkopf. “Wasserstein Auto-Encoders”. In: *International Conference on Learning Representations*. 2018.
- [23] R. Torkzadehmahani, P. Kairouz, and B. Paten. “DP-CGAN: Differentially Private Synthetic Data and Label Generation”. In: *The IEEE Conference on Computer Vision and Pattern Recognition (CVPR) Workshops*. June 2019.
- [24] Y.-X. Wang, B. Balle, and S. P. Kasiviswanathan. “Subsampled Renyi Differential Privacy and Analytical Moments Accountant”. In: *Proceedings of Machine Learning Research*. Ed. by K. Chaudhuri and M. Sugiyama. Vol. 89. Proceedings of Machine Learning Research. PMLR, Apr. 2019, pp. 1226–1235.
- [25] C. K. Williams and C. E. Rasmussen. *Gaussian processes for machine learning*. Vol. 2. 3. MIT press Cambridge, MA, 2006.
- [26] Y. Xiao, L. Xiong, and C. Yuan. “Differentially Private Data Release through Multidimensional Partitioning”. In: *Secure Data Management*. Ed. by W. Jonker and M. Petković. Berlin, Heidelberg: Springer Berlin Heidelberg, 2010, pp. 150–168.
- [27] L. Xie, K. Lin, S. Wang, F. Wang, and J. Zhou. “Differentially Private Generative Adversarial Network”. In: *CoRR* abs/1802.06739 (2018). arXiv: 1802.06739.
- [28] J. Yoon, J. Jordon, and M. van der Schaar. “PATE-GAN: Generating Synthetic Data with Differential Privacy Guarantees”. In: *International Conference on Learning Representations*. 2019.
- [29] Y.-Y. Zhang, C.-M. Shen, H. Feng, P. T. Fletcher, and G.-X. Zhang. “Generative Adversarial Networks with Joint Distribution Moment Matching”. In: *Journal of the Operations Research Society of China* 7.4 (Dec. 2019), pp. 579–597.
- [30] T. Zhu, G. Li, W. Zhou, and P. S. Yu. “Differentially Private Data Publishing and Analysis: A Survey”. In: *IEEE Transactions on Knowledge and Data Engineering* 29.8 (Aug. 2017), pp. 1619–1638.

Appendix: Differentially Private Random Feature Mean Embeddings for Synthetic Data Generation

A Background on distance measures for DP data generation

Many recent papers on DP data generation have utilized the generative adversarial networks (GAN) [8] framework, where a discriminator and a generator play a min-max form of game to optimize for the *Jensen-Shannon divergence* between the true and synthetic data distributions [16, 23, 28]. The Jensen-Shannon divergence belongs to the family of divergence, known as *Ali-Silvey distance*, *Csiszár’s ϕ -divergence* [4], defined as $D_\phi(P, Q) = \int_M \phi\left(\frac{P}{Q}\right) dQ$ where M is a measurable space and P, Q are probability distributions. Depending on the form of ϕ , $D_\phi(P, Q)$ recovers popular divergences⁵ such as the Kullback-Liebler (KL) divergence ($\phi(t) = t \log t$).

Another popular family of distance measure is *integral probability metrics (IPMs)*, which is defined by $D(P, Q) = \sup_{f \in \mathcal{F}} |\int_M f dP - \int_M f dQ|$ where \mathcal{F} is a class of real-valued bounded measurable functions on M . Depending on the class of functions, there are several popular choices of IPMs. For instance, when $\mathcal{F} = \{f : \|f\|_L \leq 1\}$, where $\|f\|_L := \sup\{|f(x) - f(y)|/\rho(x, y) : x \neq y \in M\}$ for a metric space (M, ρ) , $D(P, Q)$ yields the *Kantorovich metric*, and when M is separable, the Kantorovich metric recovers the *Wasserstein distance*, a popular choice for generative modelling such as Wasserstein-GAN and Wasserstein-VAE [2, 22]. The GAN framework with the Wasserstein distance was also used for DP data generation [6, 27].

As another example of IPMs, when $\mathcal{F} = \{f : \|f\|_{\mathcal{H}} \leq 1\}$, i.e., the function class is a unit ball in reproducing kernel Hilbert space (RKHS) \mathcal{H} associated with a positive-definite kernel k , $D(P, Q)$ yields the *maximum mean discrepancy (MMD)*, $MMD(P, Q) = \sup_{f \in \mathcal{F}} |\int_M f dP - \int_M f dQ|$. In this case finding a supremum is analytically tractable and the solution is represented by the difference in the mean embeddings of each probability measure: $MMD(P, Q) = \|\mu_P - \mu_Q\|_{\mathcal{H}}$, where $\mu_P = \mathbb{E}_{\mathbf{x} \sim \mathbb{P}}[k(\mathbf{x}, \cdot)]$ and $\mu_Q = \mathbb{E}_{\mathbf{y} \sim \mathbb{Q}}[k(\mathbf{y}, \cdot)]$. For a characteristic kernel k , the squared MMD forms a metric, i.e., $MMD^2 = 0$, if and only if $P = Q$. MMD is also a popular choice for generative modelling in the GAN frameworks [11, 12], as MMD compares two probability measures in terms of all possible moments (no information loss due to a selection of a certain set of moments); and the MMD estimator is in closed form (eq. 1) and easy to compute by the pair-wise evaluations of a kernel function using the points drawn from P and Q .

In this work, we propose to use a particular form of MMD via *random Fourier feature* representations [17] of kernel mean embeddings for DP data generation.

B Derivation of feature maps for a product of two kernels

Under our assumption, we decompose the kernel below into two kernels:

$$\begin{aligned}
& k((\mathbf{x}, \mathbf{y}), (\mathbf{x}', \mathbf{y}')) \\
&= k_{\mathbf{x}}(\mathbf{x}, \mathbf{x}') k_{\mathbf{y}}(\mathbf{y}, \mathbf{y}'), \text{ product of two kernels} \\
&\approx \left[\hat{\phi}(\mathbf{x}')^\top \hat{\phi}(\mathbf{x}) \right] \left[\mathbf{f}(\mathbf{y})^\top \mathbf{f}(\mathbf{y}') \right], \text{ random features for kernel } k_{\mathbf{x}} \\
&= \text{Tr} \left(\hat{\phi}(\mathbf{x}')^\top \hat{\phi}(\mathbf{x}) \mathbf{f}(\mathbf{y})^\top \mathbf{f}(\mathbf{y}') \right), \\
&= \text{vec}(\hat{\phi}(\mathbf{x}') \mathbf{f}(\mathbf{y}')^\top)^\top \text{vec}(\hat{\phi}(\mathbf{x}) \mathbf{f}(\mathbf{y})^\top) = \hat{\mathbf{f}}(\mathbf{x}', \mathbf{y}')^\top \hat{\mathbf{f}}(\mathbf{x}, \mathbf{y})
\end{aligned}$$

⁵See Table 1 in [14] for various ϕ divergences in the context of GANs.

C Derivation of feature maps for a sum of two kernels

Under our assumption, we compose the kernel below from the sum of two kernels:

$$\begin{aligned}
& k((\mathbf{x}_{con}, \mathbf{x}_{dis}), (\mathbf{x}'_{con}, \mathbf{x}'_{dis})) \\
&= k_{con}(\mathbf{x}_{con}, \mathbf{x}'_{con}) + k_{dis}(\mathbf{x}_{dis}, \mathbf{x}'_{dis}), \\
&\approx \hat{\phi}(\mathbf{x}_{con})^\top \hat{\phi}(\mathbf{x}'_{con}) + \frac{1}{\sqrt{d_{dis}}} \mathbf{x}_{dis}^\top \mathbf{x}'_{dis}, \\
&= \left[\frac{\hat{\phi}(\mathbf{x}_{con})}{\sqrt{d_{dis}}} \mathbf{x}_{dis} \right]^T \left[\frac{\hat{\phi}(\mathbf{x}_{con})}{\sqrt{d_{dis}}} \mathbf{x}'_{dis} \right] \\
&= \hat{\mathbf{h}}(\mathbf{x}_{con}, \mathbf{x}_{dis})^T \hat{\mathbf{h}}(\mathbf{x}_{con}, \mathbf{x}_{dis}).
\end{aligned}$$

D Sensitivity of weights

Recall that the weights are defined by $\boldsymbol{\omega} = [\omega_1, \dots, \omega_C]$, where each element is $\omega_c = \frac{m_c}{m}$. Here m_c is the number of datapoints that belong to class c and m is the total number of datapoints in the training data, i.e., $\sum_{i=1}^C m_i = m$.

When there are two datapoints' difference (denote those datapoints by $\mathbf{x}_i, \mathbf{x}'_i$) in two neighbouring datasets, there will be two classes that are affected by the two datapoints. Below, without loss of generality, we assume two datapoints difference appears in m_C and m_2 .

The sensitivity of $\boldsymbol{\omega}$ is

$$\begin{aligned}
\Delta_{\boldsymbol{\omega}} &= \max_{\mathcal{D}, \mathcal{D}'} \|\boldsymbol{\omega}(\mathcal{D}) - \boldsymbol{\omega}(\mathcal{D}')\|_2, \\
&= \max_{\mathbf{x}_i, \mathbf{x}'_i} \frac{1}{m} \left\| \begin{bmatrix} m_1 \\ m_2 \\ \dots \\ m_C(\mathbf{x}_i) \end{bmatrix} - \begin{bmatrix} m_1 \\ m'_2(\mathbf{x}'_i) \\ \dots \\ m'_C \end{bmatrix} \right\|_2, \\
&= \max_{\mathbf{x}_i, \mathbf{x}'_i} \frac{1}{m} \left\| \begin{bmatrix} 0 \\ m_2 - m'_2(\mathbf{x}'_i) \\ \dots \\ m_C(\mathbf{x}_i) - m'_C \end{bmatrix} \right\|_2, \\
&= \max_{\mathbf{x}_i, \mathbf{x}'_i} \frac{1}{m} \sqrt{|m_2 - m'_2(\mathbf{x}'_i)|^2 + |m_C(\mathbf{x}_i) - m'_C|^2}, \\
&= \frac{\sqrt{2}}{m}
\end{aligned} \tag{13}$$

where the last line is due to $\max_{\mathbf{x}'_i} |m_2 - m'_2(\mathbf{x}'_i)| = 1$ and $\max_{\mathbf{x}_i} |m_C(\mathbf{x}_i) - m'_C| = 1$.

E Sensitivity of μ_c with homogeneous data

The sensitivity of \mathbf{m}_c is

$$\begin{aligned}
\Delta_{\mathbf{m}_c} &= \max_{\mathcal{D}, \mathcal{D}'} \left\| \frac{1}{m} \sum_{i \in c_c}^m \hat{\phi}(\mathbf{x}_i) - \frac{1}{m} \sum_{i \in c_c}^m \hat{\phi}(\mathbf{x}'_i) \right\|_2, \\
&= \max_{\mathbf{x}_i, \mathbf{x}'_i} \left\| \frac{1}{m} \hat{\phi}(\mathbf{x}_i) - \frac{1}{m} \hat{\phi}(\mathbf{x}'_i) \right\|_2,
\end{aligned} \tag{14}$$

$$\leq \max_{\mathbf{x}_i} \frac{2}{m} \left\| \hat{\phi}(\mathbf{x}_i) \right\|_2, \tag{15}$$

$$\leq \frac{2}{m},$$

where the last line is because $\left\| \hat{\phi}(\mathbf{x}_i) \right\|_2 \leq 1$.

F Sensitivity of μ_c with heterogeneous data

Recall that $\hat{\mathbf{h}}(\mathbf{x}_{con}^{(i)}, \mathbf{x}_{dis}^{(i)}) = \begin{bmatrix} \hat{\phi}(\mathbf{x}_{con}^{(i)}) \\ \frac{1}{\sqrt{d_{dis}}} \mathbf{x}_{dis}^{(i)} \end{bmatrix}$ and $\mathbf{m}_c = \frac{1}{m} \sum_{i \in c}^{m_c} \hat{\mathbf{h}}(\mathbf{x}_i)$ where \mathbf{x}_i is the concatenation of $\mathbf{x}_{con}^{(i)}$ and $\mathbf{x}_{dis}^{(i)}$. The sensitivity of \mathbf{m}_c , assuming that two datasets differ at the n -th datapoint, is

$$\begin{aligned}
\Delta_{\mathbf{m}_c} &= \max_{\mathcal{D}, \mathcal{D}'} \left\| \frac{1}{m} \sum_{i \in c}^{m_c} \hat{\mathbf{h}}(\mathbf{x}_i) - \frac{1}{m} \sum_{i \in c}^{m_c} \hat{\mathbf{h}}(\mathbf{x}'_i) \right\|_2, \\
&= \max_{\mathbf{x}_n, \mathbf{x}'_n} \left\| \frac{1}{m} \begin{bmatrix} \hat{\phi}(\mathbf{x}_{con}^{(n)}) \\ \frac{1}{\sqrt{d_{dis}}} \mathbf{x}_{dis}^{(n)} \end{bmatrix} - \frac{1}{m} \begin{bmatrix} \hat{\phi}(\mathbf{x}'_{con}^{(n)}) \\ \frac{1}{\sqrt{d_{dis}}} \mathbf{x}'_{dis}^{(n)} \end{bmatrix} \right\|_2, \\
&\leq \max_{\mathbf{x}_n} \frac{2}{m} \left\| \begin{bmatrix} \hat{\phi}(\mathbf{x}_{con}^{(n)}) \\ \frac{1}{\sqrt{d_{dis}}} \mathbf{x}_{dis}^{(n)} \end{bmatrix} \right\|_2, \\
&\leq \max_{\mathbf{x}_{dis}^{(n)}} \frac{2}{m} \sqrt{1 + \frac{1}{d_{dis}} \sum_{j=1}^{d_{dis}} (\mathbf{x}_{dis,j}^{(n)})^2}, \text{ since } \|\hat{\phi}(\cdot)\|_2 = 1 \\
&\leq \frac{2\sqrt{2}}{m}, \tag{16}
\end{aligned}$$

where the last line is because \mathbf{x}_{dis} is a vector of binary variables.

G Sensitivity of $\hat{\mu}_{P_{\mathbf{x}, \mathbf{y}}}$ for image data

Using the product of two kernels

$$\begin{aligned}
\Delta_{\hat{\mu}_{P_{\mathbf{x}, \mathbf{y}}}} &= \max_{\mathcal{D}, \mathcal{D}'} \left\| \frac{1}{m} \sum_{i=1}^m \hat{\mathbf{f}}(\mathbf{x}_i, \mathbf{y}_i) - \frac{1}{m} \sum_{i=1}^m \hat{\mathbf{f}}(\mathbf{x}'_i, \mathbf{y}'_i) \right\|_2, \\
&= \max_{\mathbf{x}_n, \mathbf{x}'_n} \left\| \begin{bmatrix} \mathbf{0} & \cdots & \frac{1}{m} \hat{\phi}(\mathbf{x}_n) & \cdots & \frac{1}{m} \hat{\phi}(\mathbf{x}'_n) & \cdots & \mathbf{0} \end{bmatrix} \right\|
\end{aligned}$$

where only two columns are non-zero, as there are only two datapoints difference in two datasets if the labels of these two points are different. As the random features are norm bounded (by 1), the sensitivity is $\frac{\sqrt{2}}{m}$. On the other hand, if the labels of those two points are the same, only one column is non-zero, where the value is $\frac{1}{m} \hat{\phi}(\mathbf{x}_n) - \frac{1}{m} \hat{\phi}(\mathbf{x}'_n)$. Hence, the sensitivity is $\frac{2}{m}$. Therefore the worse case upper bound among these two cases is $\Delta_{\hat{\mu}_{P_{\mathbf{g}, \mathbf{y}}}} = \frac{2}{m}$.

H Variables in heterogeneous data are not treated as independent

While the impression may arise, our method does not assume independence between the continuous and the discrete variables and models correlations between the two types of variables implicitly. With the sum of two kernels, the embedding is a concatenation of the two: $[E_x \phi_x(x), E_y \phi_y(y)]$, where E_x means expectation wrt $p(x)$ and E_y is wrt $p(y)$. To compute $p(x)$, we need $p(y)$ with which we marginalize out y , as $p(x) = \int p(x, y) dy$. This marginalization implicitly takes into account the correlation between the two. This is less explicit than the case using the product of two kernels. However, the sum kernel is chosen for computational tractability: a sum kernel in Fourier representation has $d_x + d_y$ features while a product kernel has $d_x \cdot d_y$.

I Rényi differential privacy

Definition I.1 (α -Rényi Divergence) For two probability distributions P, Q that have the same support, the α Rényi divergence is

$$D_\alpha(P||Q) = \frac{1}{\alpha-1} \log \mathbb{E}_{x \sim Q(x)} \left(\frac{P(x)}{Q(x)} \right)^\alpha \quad (17)$$

for $\alpha \in (1, \infty)$.

J Implementation details

Our implementation, including used hyper-parameters and instructions for reproducing the experiments, will be made available upon publication. Please contact the authors for access to the code before then.

K Heterogeneous and homogenous tabular data

In this section we describe the tabular datasets we have used in our experiments with their respective sources. We include the details of data preprocessing in case it was performed on a dataset. The datasets in this form were used in all our experiments as well as the experiments on the benchmark methods.

Credit

Credit card fraud detection dataset contains the categorized information of credit card transactions which were either fraudulent or not. Ten dataset comes from a Kaggle competition and is available at the source, <https://www.kaggle.com/mlg-ulb/creditcardfraud>. The original data has 284807 examples, of which negative samples are 284315 and positive 492. The dataset has 31 categories, 30 numerical features and a binary label. We used all but the first feature (Time).

Epileptic

Epileptic dataset describes brain activity with numerical features being EEG recording at a different point in time. The dataset comes from the UCI database, <https://archive.ics.uci.edu/ml/datasets/Epileptic+Seizure+Recognition>. It contains 11500 data points, and 179 categories, 178 features and a label. The original dataset contains five different labels which we binarize into two states, seizure or no seizure. Thus, there are 9200 negative samples and 2300 positive samples.

Census

The dataset can be downloaded by means of SDGym package, <https://pypi.org/project/sdgym/>. The dataset has 199523 examples, 187141 are negative and 12382 are positive. There are 40 categories and a binary label. This dataset contains 7 numerical and 33 categorical features.

Intrusion

The dataset was used for The Third International Knowledge Discovery and Data Mining Tools Competition held at the Conference on Knowledge Discovery and Data Mining, 1999, and can be found at <http://kdd.ics.uci.edu/databases/kddcup99/kddcup99.html>. We used the file, `kddcup.data_10_percent.gz`. It is a multi-class dataset with five labels describing different types of connection intrusions. The labels were first grouped into five categories and due to few examples, we restricted the data to the top four categories.

Adult

The dataset contains information about people's attributes and their respective income which has been thresholded and binarized. It has 8049 examples, and 177 features and a binary label. The dataset can be downloaded by means of SDGym package, <https://pypi.org/project/sdgym/>.

Isolet

The dataset contains sound features to predict a spoken letter of alphabet. The inputs are sound features and the output is a latter. We binaried the labels into two classes, consonants and vowels. The dataset can be found at <https://archive.ics.uci.edu/ml/datasets/isolet>

Cervical

This dataset is created with the goal to identify the risk factors associated with cervical cancer. It is the smallest dataset with 858 instances, and 35 attributes, of which 15 are numerical and 24 are categorical (binary). The dataset can be found at <https://archive.ics.uci.edu/ml/datasets/Cervical+cancer+Risk+Factors>. The data, however, contains missing data. We followed the pre-processing suggested at <https://www.kaggle.com/saflynn/cervical-cancer-lynn> and further removed the data with the most missing values and replaced the rest with the category mean value.

Covtype

The dataset describes forest cover type from cartographic variables. The data can be found at <https://archive.ics.uci.edu/ml/datasets/covtype>. It contains 53 attributes and a multi-class label with 7 classes of forest cover types.

K.1 The training

We provide here the details of training procedure. Some of the datasets are very imbalanced, that is they contain much more examples with one label over the others. In attempt of making categories more balanced, we undersampled the class with the largest number of samples. The complexity of a dataset also determined the number of Fourier features we used. We also varied the batch size (we include the fraction of dataset used in a batch), and the number of epochs in the training. We provide the detailed parameter settings for each of the dataset in the following table.

Table 4: Parameters settings for training tabular datasets

	non-private			private			undersampling rate
	# epochs	mini-batch size	# Fourier features	# epochs	mini-batch size	# Fourier features	
adult	8000	0.1	50 000	8000	0.1	1000	0.4
census	200	0.5	10 000	2000	0.5	10 000	0.4
cervical	2000	0.6	2000	200	0.5	2000	1
credit	4000	0.6	50 000	4000	0.5	5000	0.005
epileptic	6000	0.5	100 000	6000	0.5	80 000	1
isolet	4000	0.6	100 000	4000	0.5	500	1
covtype	6000	0.05	1000	6000	0.05	1000	0.03
intrusion	10 000	0.03	2000	10 000	0.03	2000	0.1

K.2 Detailed results for binary class dataset

In the main text we included the details for a multi-class dataset and here we also include the results across all the classification methods for a binary dataset in Table 5 and Table 6. We also include the best and average F1-score over five runs for the respective classification methods in Table 7 and Table 8. Notice that this average corresponds to the average reported in Table 1 in the main text.

Table 5: Performance comparison on Credit dataset. The highest performance in five runs.

	Real		DP-CGAN (non-priv)		DP-MERF (non-priv)		DP-CGAN (1, 10 ⁻⁵)-DP		DP-MERF (1, 10 ⁻⁵)-DP	
Logistic Regression	ROC 0.95	PRC 0.91	ROC 0.83	PRC 0.37	ROC 0.92	PRC 0.79	ROC 0.74	PRC 0.52	ROC 0.78	PRC 0.61
Gaussian Naive Bayes	ROC 0.90	PRC 0.80	ROC 0.85	PRC 0.39	ROC 0.92	PRC 0.76	ROC 0.80	PRC 0.55	ROC 0.65	PRC 0.48
Bernoulli Naive Bayes	ROC 0.89	PRC 0.84	ROC 0.58	PRC 0.19	ROC 0.89	PRC 0.82	ROC 0.67	PRC 0.42	ROC 0.90	PRC 0.74
Linear SVM	ROC 0.92	PRC 0.89	ROC 0.84	PRC 0.48	ROC 0.91	PRC 0.65	ROC 0.78	PRC 0.45	ROC 0.64	PRC 0.38
Decision Tree	ROC 0.91	PRC 0.82	ROC 0.74	PRC 0.32	ROC 0.92	PRC 0.69	ROC 0.58	PRC 0.22	ROC 0.72	PRC 0.58
LDA	ROC 0.87	PRC 0.82	ROC 0.86	PRC 0.53	ROC 0.82	PRC 0.68	ROC 0.58	PRC 0.24	ROC 0.69	PRC 0.51
Adaboost	ROC 0.94	PRC 0.89	ROC 0.83	PRC 0.51	ROC 0.93	PRC 0.85	ROC 0.62	PRC 0.32	ROC 0.75	PRC 0.63
Bagging	ROC 0.91	PRC 0.84	ROC 0.79	PRC 0.42	ROC 0.91	PRC 0.79	ROC 0.57	PRC 0.21	ROC 0.74	PRC 0.61
Random Forest	ROC 0.93	PRC 0.90	ROC 0.82	PRC 0.54	ROC 0.92	PRC 0.86	ROC 0.63	PRC 0.31	ROC 0.75	PRC 0.62
GBM	ROC 0.94	PRC 0.89	ROC 0.85	PRC 0.54	ROC 0.94	PRC 0.85	ROC 0.58	PRC 0.22	ROC 0.74	PRC 0.61
Multi-layer perceptron	ROC 0.92	PRC 0.89	ROC 0.83	PRC 0.47	ROC 0.91	PRC 0.74	ROC 0.78	PRC 0.55	ROC 0.66	PRC 0.44
XGBoost	ROC 0.94	PRC 0.91	ROC 0.81	PRC 0.49	ROC 0.94	PRC 0.87	ROC 0.70	PRC 0.53	ROC 0.72	PRC 0.59
Average	0.91	0.86	0.80	0.44	0.91	0.78	0.67	0.38	0.73	0.57

Table 6: Performance comparison on Credit dataset. The average performance over five runs.

	DP-MERF (non-private)		DP-MERF (private)	
	ROC	PRC	ROC	PRC
Logistic Regression	0.919	0.808	0.796	0.665
Gaussian Naive Bayes	0.898	0.725	0.729	0.582
Bernoulli Naive Bayes	0.879	0.791	0.752	0.586
Linear SVM	0.876	0.667	0.742	0.549
Decision Tree	0.901	0.700	0.775	0.650
LDA	0.838	0.697	0.725	0.544
Adaboost	0.912	0.828	0.787	0.689
Bagging	0.909	0.805	0.811	0.709
Random Forest	0.911	0.840	0.786	0.686
GBM	0.917	0.812	0.807	0.707
Multi-layer perceptron	0.905	0.777	0.747	0.570
XGBoost	0.915	0.837	0.812	0.716
Average	0.898	0.774	0.772	0.638

Table 7: Performance comparison on Intrusion dataset. The highest performance in five runs.

	Real	DP-CGAN (non-priv)	DP-MERF (non-priv)	DP-CGAN (1, 10 ⁻⁵)-DP	DP-MERF (1, 10 ⁻⁵)-DP
Logistic Regression	0.948	0.710	0.926	0.567	0.940
Gaussian Naive Bayes	0.757	0.503	0.804	0.215	0.736
Bernoulli Naive Bayes	0.927	0.693	0.822	0.475	0.755
Linear SVM	0.983	0.639	0.922	0.915	0.937
Decision Tree	0.999	0.496	0.862	0.153	0.952
LDA	0.990	0.224	0.910	0.652	0.950
Adaboost	0.947	0.898	0.924	0.398	0.503
Bagging	1.000	0.499	0.914	0.519	0.956
Random Forest	1.000	0.497	0.941	0.676	0.943
GBM	0.999	0.501	0.924	0.255	0.933
Multi-layer perceptron	0.997	0.923	0.933	0.733	0.957
XGBoost	0.999	0.886	0.921	0.751	0.933
Average	0.962	0.622	0.900	0.526	0.875

Table 8: Performance comparison on Intrusion dataset. The average performance as F1 score over five runs.

	DP-MERF (non-private)	DP-MERF (private)
Logistic Regression	0.891	0.928
Gaussian Naive Bayes	0.845	0.792
Bernoulli Naive Bayes	0.454	0.508
Linear SVM	0.890	0.917
Decision Tree	0.911	0.907
LDA	0.859	0.925
Adaboost	0.899	0.592
Bagging	0.926	0.922
Random Forest	0.904	0.923
GBM	0.901	0.926
Multi-layer perceptron	0.898	0.941
XGBoost	0.891	0.921
Average	0.856	0.850

L Image data

L.1 Datasets

Both digit and fashion MNIST datasets are loaded through the torchvision package and used without further preprocessing. Both datasets of size 60000 consist of samples from 10 classes, which are close to perfectly balanced. Each sample is a 28x28 pixel image and thus of significantly higher dimensionality than the tabular data we tested.

L.2 Detailed results

A detailed version of the results summarized in Table 3 of the paper are shown below, for digit MNIST is Table 9 and fashion MNIST in Table 10. All scores are the average of 5 independent runs of training a generator and evaluating the synthetic data it produced. The tables show that DP-MERF consistently outperforms the other approaches across models. The only exceptions are decision trees gradient boosting and bagging, where all three models perform poorly but others do slightly better.

Table 9: Test accuracy on digit MNIST data. Average over 5 runs (data generation & model training

	Real	DP-CGAN $\epsilon = 9.6$	DP-GAN $\epsilon = 9.6$	DP-MERF $\epsilon = \infty$	DP-MERF $\epsilon = 1$	DP-MERF $\epsilon = 0.2$
Logistic Regression	0.930	0.600	0.702	0.772	0.769	0.772
Random Forest	0.969	0.638	0.538	0.714	0.685	0.702
Gaussian Naive Bayes	0.560	0.310	0.364	0.527	0.545	0.539
Bernoulli Naive Bayes	0.840	0.610	0.702	0.746	0.750	0.780
Linear SVM	0.920	0.550	0.700	0.756	0.746	0.726
Decision Tree	0.880	0.340	0.255	0.443	0.456	0.346
LDA	0.879	0.590	0.694	0.789	0.793	0.753
Adaboost	0.729	0.254	0.159	0.441	0.456	0.362
MLP	0.978	0.564	0.652	0.807	0.807	0.768
Bagging	0.928	0.430	0.282	0.624	0.602	0.508
GBM	0.909	0.460	0.205	0.678	0.659	0.552
XGBoost	0.912	0.614	0.459	0.525	0.555	0.509
Average	0.870	0.500	0.476	0.652	0.652	0.610

Table 10: Test accuracy on fashion MNIST data. Average over 5 runs (data generation & model training)

	Real	DP-CGAN $\epsilon = 9.6$	DP-GAN $\epsilon = 9.6$	DP-MERF $\epsilon = \infty$	DP-MERF $\epsilon = 1$	DP-MERF $\epsilon = 0.2$
Logistic Regression	0.844	0.461	0.626	0.725	0.728	0.714
Random Forest	0.875	0.482	0.573	0.657	0.684	0.553
Gaussian Naive Bayes	0.585	0.286	0.149	0.598	0.575	0.467
Bernoulli Naive Bayes	0.648	0.497	0.592	0.602	0.604	0.629
Linear SVM	0.839	0.389	0.613	0.685	0.684	0.697
Decision Tree	0.790	0.315	0.317	0.433	0.462	0.352
LDA	0.799	0.490	0.638	0.735	0.733	0.701
Adaboost	0.561	0.217	0.224	0.291	0.359	0.258
MLP	0.879	0.459	0.601	0.739	0.738	0.696
Bagging	0.841	0.309	0.410	0.576	0.593	0.372
GBM	0.834	0.331	0.254	0.626	0.624	0.429
XGBoost	0.826	0.489	0.478	0.596	0.610	0.445
Average	0.780	0.390	0.457	0.605	0.616	0.526